Mesomorphic glass-forming ionic complex composed of a pair of cholesterol phthalate and 1-Cn-3-methylimidazolium: Phase transition and enthalpy relaxation behavior

AUTHOR(S):

NAKAJIMA, Itaru; KITAGUCHI, Taishi; SUGIMURA, Kazuki; TERAMOTO, Yoshikuni; NISHIO, Yoshiyuki

CITATION:

NAKAJIMA, Itaru ...[et al]. Mesomorphic glass-forming ionic complex composed of a pair of cholesterol phthalate and 1-Cn-3-methylimidazolium: Phase transition and enthalpy relaxation behavior. Polymer Journal 2018, 50: 899-909

ISSUE DATE:

2018-09

URL:

http://hdl.handle.net/2433/241543

Mesomorphic glass-forming ionic complex composed of a pair of cholesterol phthalate and 1-C*n*-3-methylimidazolium: Phase transition and enthalpy relaxation behavior

Itaru Nakajima[a], Taishi Kitaguchi[a], Kazuki Sugimura[a], Yoshikuni Teramoto[b], and Yoshiyuki Nishio[a*]

[a] Division of Forest and Biomaterials Science, Graduate School of Agriculture, Kyoto University, Sakyo-ku, Kyoto 606-8502, Japan
[b] Department of Applied Life Science, Faculty of Applied Biological Sciences, Gifu University, Gifu 501-1193, Japan

Correspondence: Professor Y. Nishio, Division of Forest and Biomaterials Science, Graduate School of Agriculture, Kyoto University, Sakyo-ku, Kyoto 606-8502, Japan.
E-mail: ynishio@kais.kyoto-u.ac.jp

Running head: Ionic complex of cholesterol derivative with C*n*Mim

Abstract. Ionic complexes of a mesogenic cholesterol derivative with 1-alkyl (C*n*)-3-methylimidazolium (C*n*Mim) (*n* = 6–18) were prepared from ethanol solutions containing an equimolar mixture of cholesterol hydrogen phthalate (CHP) and [C*n*Mim][OH]; the imidazoliun hydroxide was obtained by anion exchange of [C*n*Mim][Br]. The complex samples, termed [C*n*Mim][CHP], were examined for evaluation of their thermal transition scheme. Except for two samples (*n* = 6, 8) showing no definite ordered phase, the complexes of $n \geq 10$ formed a cholesteric (*n* = 10, 12) or smectic (*n* = 14–18) mesophase in a considerably wide rage of temperature; the wider range reflects an additional thermotropic property as salts of C*n*Mim with longer alkyl chains. These fluid mesophases transformed into a mesomorphic vitreous solid without crystallization in a usual cooling process. For the glassy mesomorphic samples of selected complexes (*n* = 10, 18), the enthalpy relaxation behavior was followed as a function of the aging temperature and time, and the data were analyzed in terms of a Kohlrausch-Williams-Watts type of stretched exponential equation. Quite a narrow distribution of the relaxation time was observed for the "liquid-crystalline glasses", indicating a high uniformity of the relaxation mode.

Keywords: cholesterol derivative; imidazolium salt; ionic complex; phase transition; glassy liquid crystal; enthalpy relaxation

INTRODUCTION

Liquid-crystalline (LC) compounds of low molecular weight, which show a generally low melt viscosity, hardly vitrify and easily crystallize in a cooling process from their mesomorphic molten state. However, when the molecular weight of LC compounds is increased to ca. 500–2000 g mol^{-1} with modification using a branched structure and/or multiple mesogenic moieties, the products of medium molecular weight often form a glassy LC phase,[1–5] as a result of suppression of the crystalizability. Such mesomorphic glass-forming compounds can be applied to optical films or core elements in displays[6] and other information materials,[3,7] owing to the temperature-dependent property of changing coloration or light transmittance. For example, the vitrifiable LC compounds are promising for a rewritable recording medium; viz., some information can be transferred mechanically, electrically or photochemically to a mesophase at a temperature above the glass transition temperature (T_g), and, by simple cooling, it can be stored in the glassy state. The stored information can be erased, for instance, by isotropization at high temperatures, and then the second information can be written in

the same cycle. The vitrification phenomenon also prevails in LC polymers of higher molecular weight, and they are usable as various optical media for storing information; however, it is usually difficult to attain the fast and uniform response of the mesomorphic assembly to external stimuli, principally due to the high melt viscosity.

In an earlier study,[8] one of the authors (YN) successfully synthesized moderate molecular-weight compounds that form a glassy LC phase, without complicated procedures consuming time, namely, by a simple mixing and solvent-evaporating method. Those compounds were actually stoichiometric 1:1 complex salts composed of a cholesterol ester/aliphatic amine pair; where cholesterol hydrogen phthalate (CHP) and cholesterol hydrogen succinate (CHS) were used as the cholesterol derivative component, and a series of normal alkyl amines (C*n*-amine, *n* (carbon number) = 12–18) were employed as the aliphatic amine component. The structural formulae of the constituents are shown in Figure 1. As indicated in this figure, the complexes are stabilized by ionic interaction through salt formation between the carboxylic acid of CHP （or CHS） and the amino group of C*n*-amine. After the study of thermotropic phase behavior for the complexes, we next investigated a so-called enthalpy relaxation phenomenon resulting from physical aging of vitreous solids, using "LC glasses" of CHP/C*n*-amines each having a definite molecular weight (≤ 800).[9,10] It was observed that the distribution of the relaxation time of the CHP/C*n*-amine glasses was much narrower than that of conventional amorphous polymer glasses.

<< **Figure 1** >>

In extension of the above studies, we have lately undertaken a comparative examination using similar cholesterol-based complexes prepared by altering the ionic ingredients, to find a general tendency in thermal properties and also to suggest a practical functionality for this kind of complex materials. In the present work, the previous cation component (i.e., C*n*-amine) was replaced by 1-normal alkyl (C*n*)-3-methylimidazolium cation, $[C_nMim]^+$, to produce an ionic complex, [C*n*Mim][CHP] (see Figure 1). This cation is known as a representative component of ionic liquids (ILs) which have attracted a great deal of attention not only as a green solvent[11,12] but also as a new component of ion conductive materials.[13] Mesomorphic ILs that are capable of forming a LC phase have also been extensively studied over the past decades.[14–16] To take an advanced example of materialization, a one-dimensional ion conductive material was successfully designed by using ILs which formed a columnar LC phase.[17,18]

In this paper, we demonstrate new preparation of a LC glass-forming complex material in which the core of familiar ILs, *N*-substituted imidazolium, is incorporated. The thermotropic phase transition and enthalpy relaxation behavior of [C*n*Mim][CHP] complexes are characterized, with particular attention to the dependence on the C*n* length of the imidazolium component.

EXPERIMENTAL PROCEDURES

Original materials

Cholesterol hydrogen phthalate (CHP) was purchased from Tokyo Chemical Industry (Tokyo, Japan) and used after purification by recrystallization from ethanol solution. 1-Bromodecane, 1-bromododecane, 1-bromotetradecane and 1-bromohexadecane were purchased from Tokyo Chemical Industry, and employed without further purification. 1-Methylimidazole, 1-bromobutane, 1-bromooctane, 1-bromooctadecane, ethyl acetate, acetonitrile and ethanol (HPLC grade) were purchased from Wako Pure Chemical Industries (Osaka, Japan), and 1-bromohexane and toluene were purchased from Nacalai Tesque (Kyoto, Japan); they were all used as supplied. An ion exchange resin, Amberlite® IRA-400 (chloride form), was purchased from Sigma-Aldrich (Tokyo, Japan) and used after anion exchange from chloride to hydroxide by immersion into 1 mol L^{-1} NaOH aqueous solution.

Synthesis of 1-C*n*-3-methylimidazolium bromide ([C*n*Mim][Br]; *n* = 6–18)

All the *N*-substituted imidazolium salts used, [C*n*Mim][Br] (*n* = 6–18), were synthesized through *N*-alkylation/quaternization of 1-methylimidazole with different alkyl bromides by reference to the literature,[19,20] as follows: 1-methylimidazole (0.10 mol) was dissolved in toluene (50 mL) at ambient temperature (~25 °C), and alkyl bromide (0.15 mol) was added to the solution. The mixture was stirred at 65 °C for 24 h in a round-bottomed flask equipped with a reflux condenser under a dry N_2 atmosphere. Toluene solvent was removed by decantation (for *n* = 6 and 8) or evaporation (for *n* = 10–18), and the crude product was dissolved in acetonitrile and then dropped into ethyl acetate with vigorous stirring. After decanting of ethyl acetate, the remaining solvent was removed by heating the IL phase to 50 °C and stirring while on a vacuum line for 24 h. The salt products thus obtained were all identified as the respective objects of [C*n*Mim][Br] by ^{1}H NMR measurements (see, for example, the spectrum of [C10Mim][Br] given in Figure 4b).

Preparation of [C*n*Mim][CHP] complexes

Figure 2 shows an outline chart of the preparation route to the target complexes, [C*n*Mim][CHP], from [C*n*Mim][Br] and CHP as the starting materials.

<< **Figure 2** >>

By neutralizing amino acid with imidazolium hydroxide, Fukumoto *et al*. successfully prepared amino acid ionic liquid.[21] According to the method, we exchanged bromide ion of [C*n*Mim][Br] salts (n = 6–18) to hydroxide ion ([OH]), in advance of the complexation of imidazolium cation with carboxylate anion of CHP. Each [C*n*Mim][Br] was dissolved in ethanol at 2 wt% with stirring at room temperature (25 °C). The [C*n*Mim][Br]/ethanol solutions thus prepared were each passed through a column filled with the hydroxide-exchanged Amberlite® IRA-400, and a series of [C*n*Mim][OH]/ethanol solutions were obtained. The absence of bromine in the latter solutions was confirmed by energy dispersive X-ray analysis. Then, a weighed amount of CHP was dissolved in each [C*n*Mim][OH] solution with stirring at 25 °C for 24 h, so that the mixture contained equimolar quantities of COO^- in CHP and imidazolium cation. The mixed solutions were each poured into a glass tray and dried at 25 °C. After further drying at 40 °C *in vacuo* for 24 h, [C*n*Mim][CHP] complexes were obtained as a laminate product.

Measurements

FT-IR spectra were measured with a Shimadzu IRPrestige-21 spectrometer (Shimadzu Corporation, Kyoto, Japan). All the spectra were recorded at 20 °C in an absorption mode over a wavenumber range 400–4000 cm^{-1} with a resolution of 4 cm^{-1} via accumulation of 32 scans.

^1H NMR spectra (300 MHz) were recorded using a Varian INOVA 300 apparatus (Varian, Palo Alto, CA, USA). The measurement conditions were as follows: solvent, $CDCl_3$; solute concentration, 10 mg mL^{-1}; internal standard, tetramethylsilane (TMS); temperature, 20 °C; number of scans, 64.

Polarized optical microscopy (POM) was conducted by using an Olympus microscope (BX60F5, Olympus Corporation, Tokyo, Japan) equipped with a Mettler FP82HT/FP90 hot-stage (Mettler Toledo, Tokyo, Japan). Samples were sandwiched between a slide and cover glass.

Differential scanning calorimetry (DSC) analyses were performed on a Seiko DSC 6200/EXSTER 6000 apparatus (Seiko Instruments, Chiba, Japan). Both the

temperature and enthalpy readings were calibrated with an indium standard. A weighed amount of each sample (ca. 5 mg) was sealed in an aluminum pan. Thermograms were recorded at a scanning rate of 10 °C min^{-1} for both heating and cooling scans. The measurements were made for all the [C*n*Mim][CHP] complexes prepared above, to establish their respective phase transition schemes. Phase transition temperature and enthalpy were determined from the peak-top position and peak area, respectively, of the relevant endo- or exothermic signal appearing in thermograms. T_g was evaluated by adopting a universal method proposed by Richradson *et al.*[22,23] (see Supplementary Information), to minimize some kinetic effects due to the scanning rate and the conditions of pretreating the sample. In this purpose, the usual DSC output data of heat flow was converted into the corresponding relative enthalpy *H* and a plot of *H* against temperature was constructed. Following that, two tangential lines were drawn on both sides of the glass transition region in the *H* versus temperature curve and a value of temperature at the point of intersection was read off as T_g.

Another series of DSC measurements was carried out for selected complexes in order to evaluate the enthalpy relaxation following aging at their mesomorphic glass state. A sequence of procedure of the relaxation measurements is summarized below (see Figure 3):

1) Heating each original sample to a temperature higher than the mesophase–isotropic phase transition temperature $T_{M\text{-}I}$ by ca. 15 °C;

2) Cooling the isotropic sample at a rate of 10 °C min^{-1} to a temperature ($\approx T_g$ + 50 °C) at which the sample assumes a mesomorphic fluid state;

3) Quenching the mesomorphic sample at a rate of ~90 °C min^{-1} to an aging temperature T_a ($< T_g$);

4) Aging the glassy sample at T_a over a time period t_a in the DSC cell (t_a < 1 h) or in a thermo-regulated incubator (NCB-3200, Tokyo Rikakikai, Tokyo, Japan) ($t_a \geq 1$ h);

5) Quenching the aged sample from T_a to −60 °C;

6) Heating the frozen sample at a rate of 10 °C min^{-1} from −60 °C to a temperature above T_g.

<< **Figure 3** >>

RESULTS AND DISCUSSION

Formation of ionic complex

Confirmation of ionic complex formation was made for [C*n*Mim][CHP] samples by ^{1}H

NMR and FT-IR measurements. Figure 4 illustrates a ^{1}H NMR spectrum of [C10Mim][CHP] (part (a)) in comparison with that of [C10Mim][Br] (part (b)). The composition of this complex sample was evaluated as [C10Mim]/[CHP] = 0.99 using the peak intensities of signals **a** and **e** for the C10Mim component and those of signals **3'** and **6'** for the CHP component. In a similar manner of calculation, all the samples with various alkyl chain lengths (*n* = 6–18) showed a stoichiometric ratio of [C*n*Mim]/[CHP] = 1.00 ± 0.04. Furthermore, it was observed that the chemical shift value of an imidazolium proton (signal **d**) of [C*n*Mim][CHP] was always larger by ca. 0.5 ppm than the corresponding value of [C*n*Mim][Br]. In the two spectra given in Figure 4, we find the proton signal concerned at 11.2 ppm for [C10Mim][CHP] and at 10.6 ppm for [C10Mim][Br]. A similar shift of the imidazolium proton signal toward the lower magnetic field has been noted for [C*n*Mim][Ac] (Ac, CH_3COO^-) prepared from [C*n*Mim][Br].[24,25] By analogy with this, it may be inferred that the [C*n*Mim][CHP] samples are a 1:1 type of complex compound linked through a salt formation of imidazolium carboxylate.

<< **Figure 4** >>

Figure 5 displays FT-IR spectra of CHP, [C10Mim][CHP] and [C10Mim][Br] as reference. In the spectral data (a) of CHP *per se*, there appear a C=O stretching band at 1701 cm^{-1} and a C-O stretching band at 1310 cm^{-1}, both associated with a carboxylic acid dimer. The other major bands observed at 1735 and 1255 cm^{-1} signalize the ester linkage of cholesterol with phthalic acid in CHP. In the data (b) of [C10Mim][CHP], there is no absorption signal of the carboxylic acid. Instead of this disappearance, absorption bands signalizing carboxylate formation emerge at 1590 and 1370 cm^{-1} in the spectrum (b). These pieces of evidence ensure the complete complexation between the two ionic constituents, $[C10Mim]^+$ and $[CHP]^-$. Similar FT-IR observations were made for the other [C*n*Mim][CHP] samples. The formal feature of the complexes may be like a fatten tadpole-shape, as modeled in Figure 2; the cholesteryl group is articulated with the C*n* tail through a somewhat bulky joint comprising phthaloyl and imidazolium moieties.

<< **Figure 5** >>

Thermal transition scheme

Thermal transition behavior of CHP is well established in earlier studies.[8–10] The

transition scheme was essentially reproduced in the present DSC measurement: On heating the original crystalline CHP obtained from ethanol solution, it melted at 169 °C to transform into an isotropic liquid (I). When the molten CHP was cooled, the isotropic phase changed into a cholesteric mesophase (M_{Ch}) at ~85 °C. Upon continued cooling of the mesomorphic CHP, it was vitrified at ca. 30 °C without crystallizing and with retaining a cholesteric planar texture. In the second heating scan, the anisotropic glass (G_{Ch}) changed again into the fluid mesophase around 30 °C and then transformed into the isotropic liquid at ~92 °C. In the following cycles of cooling and heating, CHP showed the same enantiotropic phase behavior, $I \leftrightarrow M_{Ch} \leftrightarrow G_{Ch}$ (see the first row of data listed in Table 1). It should be remarked here that the CHP molecules with a steroid mesogen are dimerized through dual intermolecular hydrogen bonding between the COOH groups at their terminal ends (see Figure 2), and this dimer is a structural unit involved in the observed phase behavior.

Similar DSC experiments were conducted for the tadpole-shaped [C*n*Mim][CHP] complexes; the samples were all prepared as a crystalline material from ethanol solution. After isotropization of each sample by heating to a high temperature (>120 °C), the thermotropic phase behavior was evaluated in the subsequent cooling and heating cycles. The results are summarized in Table 1 and representative DSC data are compiled in Figure 6. Roughly we observed three patterns (A, B and C) of phase transition scheme, which varied depending on the alkyl chain length (*n*) of $[CnMim]^+$.

<< **Table 1** >>

<< **Figure 6** >>

Pattern A refers to thermal behavior of the complexes of n = 6 and 8. These samples exhibited only a glass transition (T_g < ca. 10 °C) and no phase transition accompanied by an exo- or endo-thermic signal in the ordinary DSC cycles, as the evidence is illustrated for [C8Mim][CHP] in Figure 6a. Thus these complexes solely repeated the transition behavior, $I \leftrightarrow G_A$ (amorphous glass).

In pattern B, two mesomorphic phases appear before glass transition in the cooling process from an isotropic molten state, and consecutive crystallization and fusion take place before isotropization in the heating process from a mesomorphic glass state. This pattern refers to thermal behavior of the complexes of n = 10 and 12. Figure 6b illustrates DSC thermograms of [C10Mim][CHP], together with supplementary POM photographic data. In the cooling scan, first the isotropic melt (I) transformed into a

cholesteric mesophase (M_{Ch}) at 81 °C and then this phase partly changed into a smectic mesophase (M_{Sm}) at 26 °C, followed by vitrification into a mesomorphic glass ($G_{Ch/Sm}$) at ca. 10 °C. This specification of the mesophases can be supported by the data of transition enthalpy (included in Figure 6b, left), and by the POM observations as well. In Figure 6b, right, the upper POM image shows a cholesteric planar texture and the lower image contains a battonet-like texture mingled with the planar one. In the subsequent heating scan, the anisotropic glass unfroze into a fluid mesophase ($M_{Ch/Sm}$) above 10 °C, and right after transition of $M_{Ch/Sm} \rightarrow M_{Ch}$ at 32 °C, a cold crystallization occurred at 40–50 °C from the M_{Ch} state. Then the resulting crystal (K) melted in a temperature range 60–90 °C and ultimately transformed again into the isotropic fluid. Concerning [C12Mim][CHP], the scheme of "I → M_{Ch} →$M_{Ch/Sm}$ → $G_{Ch/Sm}$" was also applicable to the cooling process of this sample, but, in the heating, a cold crystallization occurred at 45–65 °C from the $M_{Ch/Sm}$ state that was unfrozen above ~13 °C from the $G_{Ch/Sm}$ state. Following fusion at 70–90 °C of the formed crystal (K), the M_{Ch} phase was restored and it transformed into the isotropic melt at 123 °C.

Pattern C is classified as an enantiotropic scheme, I ↔ M_{Sm} ↔ G_{Sm}, and refers to thermal behavior of the complexes of n = 14–18. Examples of DSC thermograms are given in Figure 6c and d for [C14Mim][CHP] and [C18Mim][CHP], respectively. An isotropic liquid–mesophase transition (at >150 °C) and a single glass transition ($T_g \lesssim$ 5 °C) are clearly observed in both cooling and heating scans for these samples. The temperature range where the complexes are in a liquid-crystalline state is extremely wide. On examination by POM, a battonet texture (Figure 6c, right) or a fan-shaped texture (Figure 6d, right) was observed in their mesomorphic fluid states. These optical images are characteristic of the smectic type of liquid crystals. It was also perceived that the complexes generally preferred a molecular arrangement to orient perpendicular rather than parallel to the surface plane of a slide glass in the mesomorphic state. This tendency may be ascribed to a homeotropic character of the Cn chain ($n \geq 14$) serving as a considerably long tail of the complexes.

To survey the results listed in Table 1, we can make the following remarks: (1) [CnMim][CHP] complexes form a mesophase and solidify into a mesomorphic glass (or liquid-crystalline glass) upon cooling, except for the samples of n = 6 and 8. However, even the latter two would intrinsically have an ability of forming a mesophase (according to quite a slower kinetics), which was suggested by microscopic observation of a feeble birefringent phase for the samples annealed at ~50 °C for more than 5 h. (2) The mesophase of [CnMim][CHP] tends to be more ordered with increasing length of the Cn chain (see $\Delta H_{M\text{-}I}$ data in Table 1); the molecular arrangement therein is

dominantly cholesteric for n = 10 and 12, and smectic for n = 14–18. (3) T_g of [CnMim][CHP] tends to decrease with an increase in n and is always lower than that of CHP. In contrast, the phase transition temperature $T_{M\text{-}I}$ increases with increasing n (≥ 10). In particular, the values (122–165 °C) for the complexes of n ≥ 12 are extraordinarily high, beyond that (92.0 °C) for CHP.

The Cn-length dependence of the thermal behavior of [CnMim][CHP] is roughly similar in a broad outline to that examined formerly for CHP/Cn-amine complexes.[8,10] In the latter system, however, the scheme of I ↔ M_{Sm} ↔ G_{Sm} (pattern C) was applicable to the complexes with Cn-amines of n = 10–18, and CHP/C8-amine provided a transition scheme of I ↔ M_{Ch} ↔ G_{Ch} while CHP/C6-amine obeyed the scheme of I ↔ G_A (pattern A). Thus the ordered phases, M_{Sm} and M_{Ch}, were formed using relatively shorter Cn chains, compared with the situation in the [CnMim][CHP] system. Furthermore, $T_{M\text{-}I}$ values (ca. 85–100 °C)[8] observed for CHP/Cn-amine samples of n ≥ 12 were noticeably lower than those of [CnMim][CHP]s with the same range of Cn length and rather comparable to that of CHP *per se*. The very high $T_{M\text{-}I}$ values of the [CnMim][CHP] complexes might strongly reflect a thermotropic property as *N*-substituted imidazolium IL, although there would be a contribution of an increase in the axial ratio of the mesogenic moiety of the complexes with the rigid imidazolium ring. According to literature,[14,26–28] salts of [CnMim]$^+$ with longer alkyl chains (n = 12–18) are usually crystalline at room temperature and often exhibit a liquid-crystalline (smectic) phase in the molten state; for instance, [CnMim][Br] of n ≥ 12 show transitions of K → M_{Sm} at 50 °C or thereabouts and M_{Sm} → I at temperatures much higher than 100 °C.[27,28]

Enthalpy relaxation of mesomorphic glasses

The physical aging of glassy materials, generally occurring during their annealing at temperatures lower than T_g, is interpreted as a spontaneous non-equilibrium phenomenon. More specifically, when a viscous fluid is vitrified below T_g by cooling, excess quantities of volume and enthalpy carried over in the solid should be decrease with time toward the respective equilibrium values at the aging temperature. This behavior is commonly designated as volume relaxation or enthalpy relaxation,[29,30] often attended by serious changes in mechanical property and endurance of the material.[31–34] In the present paper, our interest was focused on the enthalpy relaxation behavior of mesomorphic vitreous solids from a fundamental standpoint. The samples explored herein were the vitrified [CnMim][CHP]s of n = 10 and 18 retaining cholesteric and smectic mesomorphies, respectively.

The enthalpy relaxation of glassy materials can be observed as an endothermic peak in their DSC thermograms just after the onset of the glass transition when the aged samples are heated. Figure 7 illustrates DSC thermograms obtained for the [C18Mim][CHP] LC glass which was aged for different time periods at −10 °C. The enthalpy ΔH can be evaluated from the endothermic peak area shaded in each thermogram. Deservedly, the area increased with aging time, accompanied by a systematic shift in the peak-top position and also in the onset point of the glass transition to the side of higher temperature. Figure 8 collects data of the time evolution of ΔH for the glassy complex aged at various temperatures. The enthalpy rose rapidly with time in a relatively early stage of the aging and eventually leveled off to converge at an equilibrium ΔH_∞, the value of which became larger as the aging temperature was lowered. A similar tendency of the dependence of ΔH on aging time (t_a) and temperature (T_a) was observed for the [C10Mim][CHP] LC glass.

<< **Figure 7** >>

<< **Figure 8** >>

Regression analysis of the ΔH versus t_a plots was made by the following Kohlrausch-Williams-Watts (KWW) type of equation with a stretched exponential term:[35]

$$\Delta H = \Delta H_\infty [1 - \exp\{-(t_a/\tau)^\beta\}] \qquad (1)$$

where τ is the relaxation time of enthalpy and β is a non-exponential parameter ($0 < \beta \leq 1$) indicating the degree of distribution of the relaxation time. Table 2 collects values of τ and β determined by the best fitting to the ΔH data observed for the present complex glasses of n = 10 and 18.

<< **Table 2** >>

In Figure 9a, the logarithmic plot of τ against the reciprocal of aging temperature (in K) is constructed for the two glassy complexes. For both complexes, the plot provided a good linearity indicating applicability of the Arrhenius equation:

$$\tau^{-1} = \tau_0^{-1} \exp[-E_a/(RT)] \qquad (2)$$

where E_a is the activation energy for the enthalpy relaxation process in the glassy state, and τ_0^{-1} and R are the pre-exponential factor and the gas constant, respectively. Then the energy E_a can be evaluated from the slope of each straight line of the plot. The

result of the evaluation is listed in Table 2. Figure 9b shows another plotting with ordinary logarithm of τ against the inverse of a T_g-reduced aging temperature for the mesomorphic glasses. According to Angell,[36] the fragility of glassy materials is generally defined in the following way:

$$m = d\log\tau / d(T_g/T) \mid_{T = T_g} \qquad (3)$$

where m is the fragility index and its larger value denotes higher fragility. Table 2 also lists m data estimated from the slope of each Angel plot that gives linearity in Figure 9b.

<< **Figure 9** >>

Table 2 includes results of similar relaxation analysis performed for LC glasses of CHP and CHP/C*n*-amine (n = 10, 16, 18).[9,10] In comparison with the previous results, the following remarks should be made on the enthalpy relaxation data for the present complex glasses:

(1) The parameter β was again of a higher value, situated at 0.90 and 0.84 on average for n = 10 and 18, respectively. In principle, the extreme of β = 1 means that there occurs just a single (or unified) relaxation mode, while, when the distribution of the relaxation time is very broad due to concurrence of many relaxation modes in the aging process, β assumes a much smaller value to approach zero. As can be seen from Table 2, the β values for the cholesterol-based LC glasses explored so far are all considerably larger than those (mostly 05–0.55)[37] reported for conventional amorphous polymers. Another notice is that the ionic complexes of CHP with C*n*-amine and C*n*Mim provided somewhat higher β values relative to that (~0.7) observed for the neat CHP (dimer) system.

(2) The relaxation times of the [C*n*Mim][CHP] glasses were roughly several to 40 times longer than those of the CHP/C*n*-amine glasses. Values of E_a estimated for the former glasses were higher than those for the latter ones, when compared between the samples having the same C*n* length. With regard to the [C*n*Mim][CHP] glasses, the bulkiness of the ionic junction involving an imidazolium moiety might lower the molecular mobility in the relaxation process. In any of the two complex series, however, the E_a values are much lower than those (426–1070 kJ mol^{-1})[38,39] reported for poly(styrene).

(3) The fragility index m and also E_a for the [C*n*Mim][CHP] glasses decreased with an increase of the C*n* length, as in the case for the CHP/C*n*-amine glasses. Both the values for the two series of ionic complex were evidently lower than those for CHP *per se*. However, the estimations for [C10Mim][CHP] yielded somewhat larger m and E_a,

each approaching the data for CHP, which may be attributable to an additional factor, i.e., the prevalence of cholesteric ordering rather than of smectic one. In any case, the C*n* tail of the respective cationic components exercised an effect of diluent solvent for the molecular assembly to promote cooperative motions. This should allow the glassy materials to be less fragile. Interestingly, the present result is in accordance with a general trend pointed out by Böhmer:[40] viz., the distribution of the relaxation time is rather wider (i.e., β is lower) as the glassy material concerned is more fragile.

CONCLUSION

Stoichiometric 1:1 ionic complexes, [C*n*Mim][CHP] (n = 6–18), were successfully prepared from ethanol solutions containing an equimolar mixture of cholesterol hydrogen phthalate (CHP) and 1-C*n*-3-methylimidazolium hydroxide ([C*n*Mim][OH]). The hydroxide was derived from [C*n*Mim][Br] by exchange of the anion. The structural feature of the complexes is a fatten tadpole-shape; the mesogenic cholesteryl group is articulated with the C*n* tail through a bulky joint comprising phthaloyl and imidazolium moieties. Thermal properties involving liquid crystallinity of the ionic complexes were investigated in comparison with the previous result for a series of CHP/C*n*-amine.

Concerning the transition behavior after isotropizing treatment, the [C*n*Mim][CHP] complexes formed a mesophase and solidified into a mesomorphic glass upon cooling, except for the samples of n = 6 and 8. The detected mesophase tended to be more ordered with increasing length of the C*n* chain; the molecular arrangement therein was dominantly cholesteric for n = 10 and 12, and smectic for n = 14–18. The values of isotropic transition point (i.e., $T_{M\text{-}I}$) observed for the samples of $n \geq 12$ were much higher than those of CHP/C*n*-amine complexes with the corresponding range of C*n* length. The marked elevation in $T_{M\text{-}I}$ of the [C*n*Mim][CHP] complexes can be interpreted as due to an additional thermotropicity as imidazolium salts with longer *N*-alkyl substituents.

For the mesomorphic glasses of [C*n*Mim][CHP] (n = 10 and 18), the enthalpy relaxation behavior was monitored as evolution of a DSC endothermic peak, and the data analysis was made in terms of the KWW type of stretched exponential function. Of significance was the confirmation of extremely narrow distribution of the relaxation time from the estimation of the exponent β close to unity. The activation energy E_a for the relaxation process and the fragility index m were also evaluated from the Arrhenius and Angell equations, respectively. The obtained E_a and m values were appreciably

higher compared to those for the vitreous CHP/C*n*-amine samples with the corresponding C*n* length. This indicates that the bulkiness of the ionic junction comprising the imidazolium moiety lowered the molecular mobility in the relaxation process.

The present study should serve as a helpful guide for designing functional LC materials possessing vitrifiability. The thermal and optical properties of the cholesterol-based complexes may be variable not only by altering a part of the ionic junction but also by modifying the alkyl tail of the counter component. In the meanwhile, the enthalpy relaxation analysis for the mesomorphic glasses provides useful information in understanding the physical aging of polymer glasses (involving both amorphous and liquid-crystalline glasses[39,41]). The present result would still reflect a generic property of low or medium molecular-weight compounds. In this respect, we will be required to complement further relaxation data using polymers having a similar complex structure as a pendant group; this is currently under way in our laboratory.

ACKNOWLEDGEMENTS

This work was partially financed by a Grant-in-Aid for Scientific Research (A) (No. 26252025 to Y.N.) from the Japan Society for the Promotion of Science.

CONFLICT OF INTEREST

The authors declare no conflict of interest.

REFERENCES

1. Tsuji, K., Sorai, M. & Seki, S. New finding of glassy liquid crystal – a non-equilibrium state of cholesteryl hydrogen phthalate. *Bull. Chem. Soc. Jpn.* **44,** 1452–1452 (1971).
2. Wedler, W., Demus, D., Zaschke, H., Mohr, K., Schäfer, W. & Weissflog, W. Vitrification in low-molecular-weight mesogenic compounds. *J. Mater. Chem.* **1,** 347–356 (1991).
3. Tamaoki, N. Cholesteric liquid crystals for color information technology. *Adv. Mater.* **13,** 1135–1147 (2001).
4. Chen, S. H., Shi, H., Conger, B. M., Mastrangelo, J. C. & Tsutsui, T. Novel

vitrifiable liquid crystals as optical materials. *Adv. Mater.* **8,** 998–1001 (1996).

5. Fan, F. Y., Culligan, S. W., Mastrangelo, J. C., Katsis, D., Chen, S. H. & Blanton, T. N. Novel glass-forming liquid crystals. 6. High-temperature glassy nematics. *Chem. Mater.* **13,** 4584–4594 (2001).
6. Van De Witte, P. & Lub, J. Optical components from a new vitrifying liquid crystal. *Liq. Cryst.* **26,** 1039–1046 (1999).
7. Tamaoki, N., Aoki, Y., Moriyama, M. & Kidowaki, M. Photochemical phase transition and molecular realignment of glass-forming liquid crystals containing cholesterol/azobenzene dimesogenic compounds. *Chem. Mater.* **15,** 719–726 (2003).
8. Kimura, N., Takeshima, N., Nishio, Y. & Suzuki, H. Phase behavior of novel liquid-crystalline salts containing a cholesteryl group. *Mol. Cryst. Liq. Cryst.* **287,** 35–45 (1996).
9. Yoshio, M., Miyashita, Y. & Nishio, Y. Enthalpy relaxation behavior of liquid-crystalline glasses of an esterified cholesterol derivative and its complex salts with aliphatic amines. *Mol. Cryst. Liq. Cryst.* **357,** 27–42 (2001).
10. Nishio, Y. & Chiba, R. Structural characteristics and novel functionalisation of liquid-crystalline polysaccharides and cholesterol derivatives. *Ekisho* **7,** 218–227 (2003).
11. Welton, T. Room-temperature ionic liquids. Solvents for synthesis and catalysis. *Chem. Rev.* **99,** 2071–2083 (1999).
12. Hallett, J. P. & Welton, T. Room-temperature ionic liquids: solvents for synthesis and catalysis. 2. *Chem. Rev.* **111,** 3508–3576 (2011).
13. Armand, M., Endres, F., MacFarlane, D. R., Ohno, H. & Scrosati, B. Ionic-liquid materials for the electrochemical challenges of the future. *Nat. Mater.* **8,** 621–629 (2009).
14. Binnemans, K. Ionic liquid crystals. *Chem. Rev.* **105,** 4148–4204 (2005).
15. Axenov, K. V. & Laschat, S. Thermotropic ionic liquid crystals. *Materials* **4,** 206–259 (2011).
16. Goossens, K., Lava, K., Bielawski, C. W. & Binnemans, K. Ionic liquid crystals: versatile materials. *Chem. Rev.* **116,** 4643–4807 (2016).
17. Yoshio, M., Mukai, T., Ohno, H. & Kato, T. One-dimensional ion transport in self-organized columnar ionic liquids. *J. Am. Chem. Soc.* **126,** 994–995 (2004).
18. Shimura, H., Yoshio, M., Hoshino, K., Mukai, T., Ohno, H. & Kato, T. Noncovalent approach to one-dimensional ion conductors: enhancement of ionic conductivities in nanostructured columnar liquid crystals. *J. Am. Chem. Soc.* **130,**

1759–1765 (2008).

19. Bonhôte, P., Dias, A.-P., Papageorgiou, N., Kalyanasundaram, K. & Grätzel, M. Hydrophobic, highly conductive ambient-temperature molten salts. *Inorg. Chem.* **35,** 1168–1178 (1996).
20. Huddleston, J. G., Visser, A. E., Reichert, W. M., Willauer, H. D., Broker, G. A. & Rogers, R. D. Characterization and comparison of hydrophilic and hydrophobic room temperature ionic liquids incorporating the imidazolium cation. *Green Chem.* **3,** 156–164 (2001).
21. Fukumoto, K., Yoshizawa, M. & Ohno, H. Room temperature ionic liquids from 20 natural amino acids. *J. Am. Chem. Soc.* **127,** 2398–2399 (2005).
22. Richardson, M. J. & Savill, N. G. Derivation of accurate glass transition temperatures by differential scanning calorimetry. *Polymer* **16,** 753–757 (1975).
23. Kimura, N., Aizawa, K., Nishio, Y. & Suzuki, H. Determination of glass transition temperature by differential scanning calorimetry. *Kobunshi Ronbunshu* **53,** 866–868 (1996).
24. Vitz, J., Erdmenger, T., Haensch, C. & Schubert, U. S. Extended dissolution studies of cellulose in imidazolium based ionic liquids. *Green Chem.* **11,** 417–424 (2009).
25. Matthews, R. P., Villar-Garcia, I. J., Weber, C. C., Griffith, J., Cameron, F., Hallett, J. P., Hunt, P. A. & Welton, T. A structural investigation of ionic liquid mixtures. *Phys. Chem. Chem. Phys.* **18,** 8608–8624 (2016).
26. Bowlas, C. J., Bruce, D. W. & Seddon, K. R. Liquid-crystalline ionic liquids. *Chem. Commun.* 1625–1626 (1996).
27. Bradley, A. E., Hardacre, C., Holbrey, J. D., Johnston, S., McMath, S. E. J. & Nieuwenhuyzen. Small-angle X-ray scattering studies of liquid crystalline 1-alkyl-3-methylimidazolium salts. *Chem. Mater.* **14,** 629–635 (2002).
28. Getsis, A. & Mudring, A. -V. Imidazolium based ionic liquid crystals: structure, photophysical and thermal behaviour of $[C_n\text{mim}]\text{Br}\cdot x\text{H}_2\text{O}$ (n = 12, 14; x = 0, 1). *Cryst. Res. Technol.* **43,** 1187–1196 (2008).
29. Weitz, A. & Wunderlich, B. Thermal analysis and dilatometry of glasses formed under elevated pressure. *J. Polym. Sci. Polym. Phys. Ed.* **12,** 2473–2491 (1974).
30. Cowie, J. M. G. & Ferguson, R. Physical aging studies in poly(vinyl methyl ether). 1. Enthalpy relaxation as a function of aging temperature. *Macromolecules* **22,** 2307–2312 (1989).
31. Mininni, R. M., Moore, R. S., Flick, J. R. & Petrie, S. E. B. The effect of excess volume on molecular mobility and on the mode of failure of glassy poly(ethylene

terephthalate). *J. Macromol. Sci. Part B* **8,** 343–359 (1973).

32. Cavaille, J. Y., Etienne, S., Perez, J., Monnerie, L. & Johari, G. P. Dynamic shear measurements of physical ageing and the memory effect in a polymer glass. *Polymer* **27,** 686–692 (1986).
33. Bauwens-Crowet, C. & Bauwens, J.-C. Annealing of polycarbonate below the glass transition temperature up to equilibrium: A quantitative interpretation of enthalpy relaxation. *Polymer* **27,** 709–713 (1986).
34. Struik, L. C. E. *Physical aging in amorphous polymers and other materials*. (Elsevier Scientific Pub. Co., Amsterdam, Netherland, 1978).
35. Williams, G. & Watts, D. C. Non-symmetrical dielectric relaxation behaviour arising from a simple empirical decay function. *Trans. Faraday Soc.* **66,** 80–85 (1970).
36. Angell, C. A. Relaxation in liquids, polymers and plastic crystals — strong/fragile patterns and problems. *J. Non. Cryst. Solids* **131–133,** 13–31 (1991).
37. Yoshida, H. Enthalpy relaxation and fragility of amorphous polymers. *Kobunshi Ronbunshu* **53,** 874–876 (1996).
38. Yoshida, H. Enthalpy relaxation of polymeric glasses. *Netsu Sokutei* **13,** 191–199 (1986).
39. Tanaka, Y. & Udagawa, H. Structural relaxation of a side-chain type liquid crystalline polymer having longer spacer chain: Analysis of enthalpy relaxation with an activation energy specrum. *Kobunshi Ronbunshu* **66,** 463–469 (2009).
40. Böhmer, R. Non-linearity and non-exponentiality of primary relaxations. *J. Non. Cryst. Solids* **172–174,** 628–634 (1994).
41. Tokita, M., Funaoka, S. & Watanabe, J. Study on smectic liquid crystal glass and isotropic liquid glass formed by thermotropic main-chain liquid crystal polyester. *Macromolecules* **37,** 9916–9921 (2004).

Supplementary Information accompanies the paper on Polymer Journal website (http://www.nature.com/pj)

Titles and legends to figures

Figure 1 Structural formulae of the cholesterol-based ionic complexes, CHP (or CHS)/C*n*-amine (studied previously[8–10]) and [C*n*Mim][CHP] (targeted in the present paper).

Figure 2 Outline chart showing the preparation route to [C*n*Mim][CHP] samples (n = 6–18) from [C*n*Mim][Br] and CHP.

Figure 3 Thermal program of the DSC measurement for enthalpy relaxation experiment. Abbreviations: $T_{M\text{-}I}$, mesophase–isotropic phase transition temperature; T_g, glass transition temperature; T_a, aging temperature; t_a, aging time.

Figure 4 ^{1}H NMR spectra of (a) [C10Mim][CHP] and (b) [C10Mim][Br] in $CDCl_3$. Notations: †, proton signals in multitude from a steroid group of $[CHP]^-$ and f–n positions of $[C10Mim]^+$; ‡, proton signals in multitude from a benzene ring of $[CHP]^-$ and b and c positions of $[C10Mim]^+$. Peak integral values used for calculation of the complex composition (in (a)) are as follows: **a**, 42.12; **e**, 29.04; **3'**, 14.49; **6'**, 14.35.

Figure 5 FT-IR spectra of (a) CHP *per se*, (b) [C10Mim][CHP] and (c) [C10Mim][Br]. Spectra (a) and (b) were measured by the standard KBr-pellet method. Spectrum (c) was recorded by a liquid-layer method in which the fluid sample was sandwiched between two KBr plates.

Figure 6 DSC thermograms and POM images of selected [C*n*Mim][CHP] samples: (a) [C8Mim][CHP]; (b) [C10Mim][CHP]; (c) [C14Mim][CHP]; (d) [C18Mim][CHP]. The thermograms were all recorded at a scanning rate of 10 °C min^{-1} after isotropization of each sample by heating to a temperature of >120 °C. POM images were captured at various temperatures in the cooling process. Particularly, the image in Figure 6c was obtained by tilting the sample slide on the POM stage. Abbreviations: K, crystal; M, mesophase; G, glassy state; A, amorphous; Ch, cholesteric; Sm, smectic.

Figure 7 DSC thermograms for the LC glass of [C18Mim][CHP], each obtained after aging for the indicated time period at −10 °C. The data were recorded in the heating scan at 10 °C min^{-1}. Solid arrows indicate the onset point of the glass transition, and a

white arrow indicates the T_g position determined by a universal method proposed by Richardson *et al*.[22,23]

Figure 8 Time evolution of enthalpy relaxation for the LC glass of [C18Mim][CHP] which was aged at different temperatures lower than T_g.

Figure 9 (a) Arrhenius plots of the relaxation time against the reciprocal of aging temperature and (b) Angell plots of the relaxation time against the inverse of T_g-reduced aging temperature, constructed for LC glasses of [C10Mim][CHP] and [C18Mim][CHP].

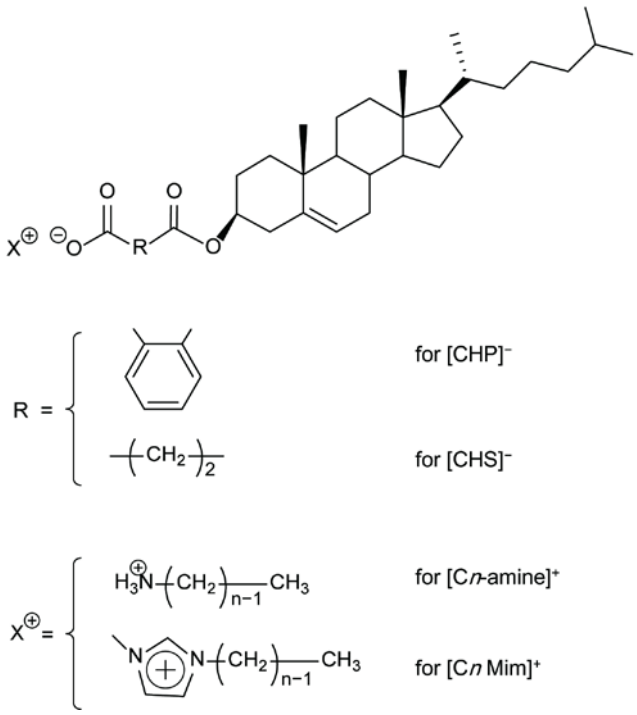

Figure 1

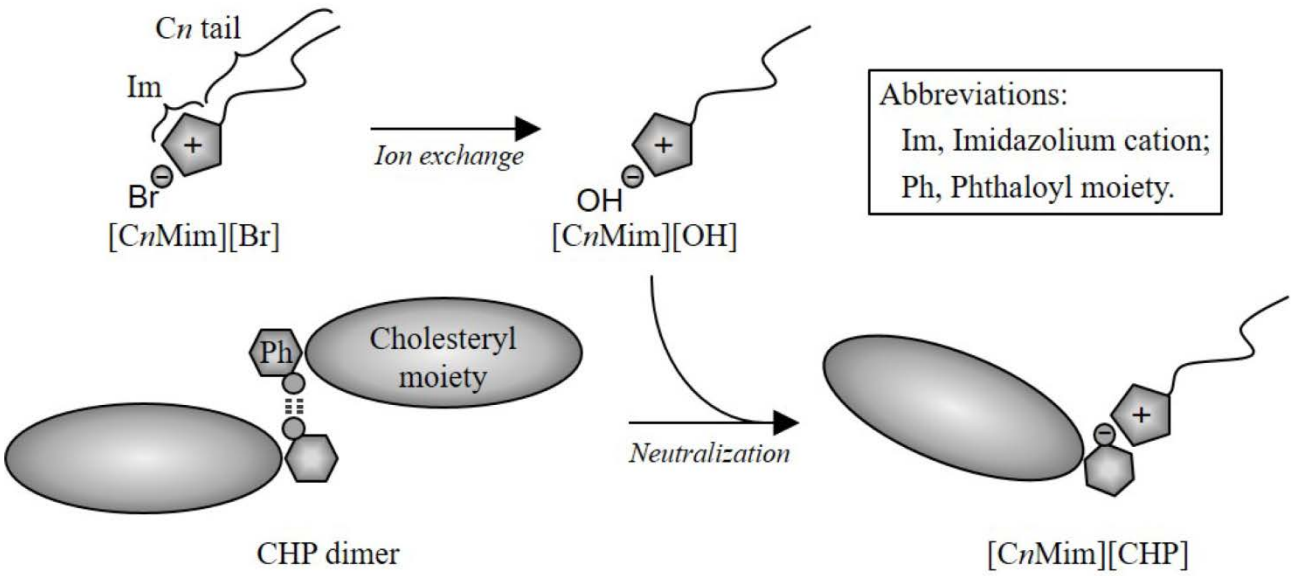

Figure 2

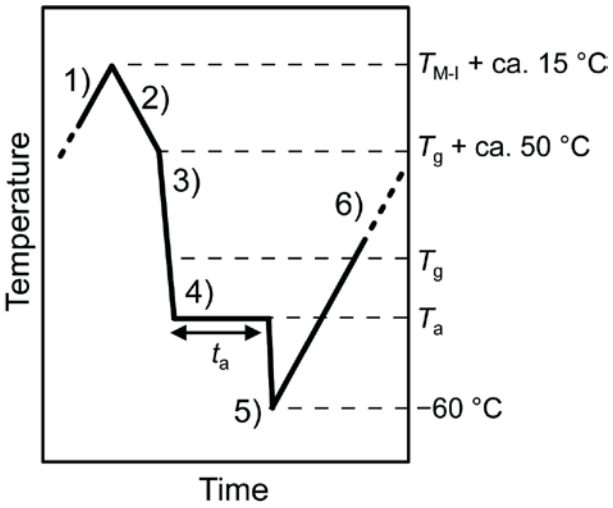

Figure 3

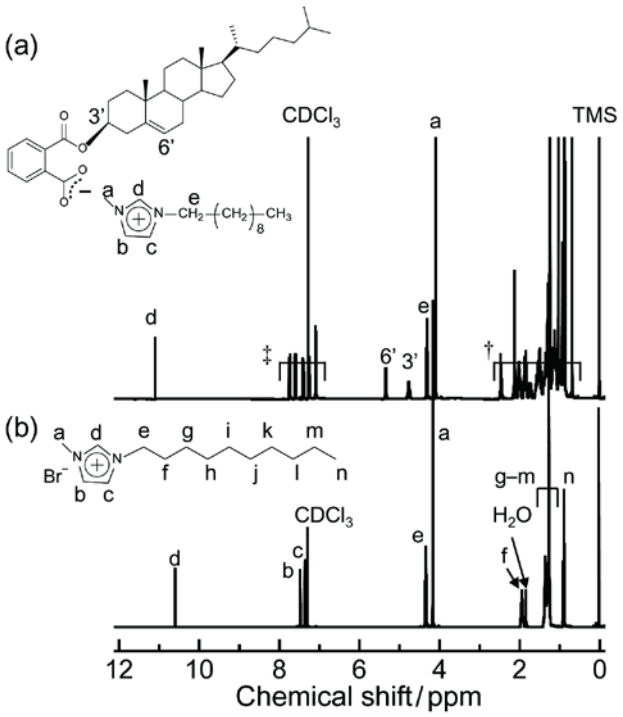

Figure 4

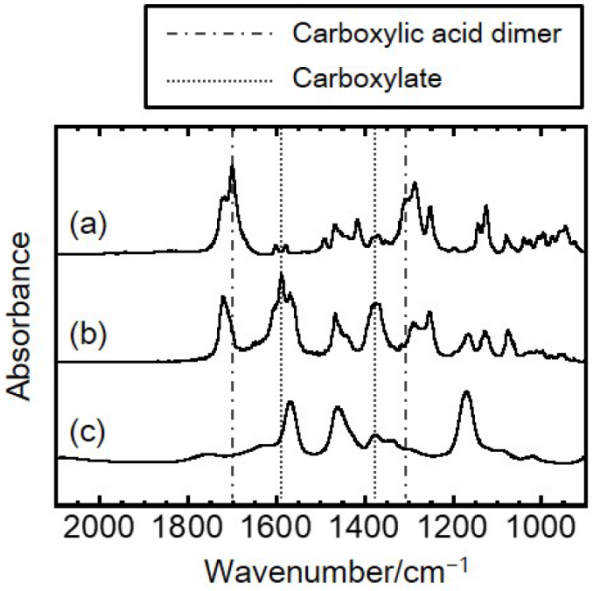

Figure 5

(a)

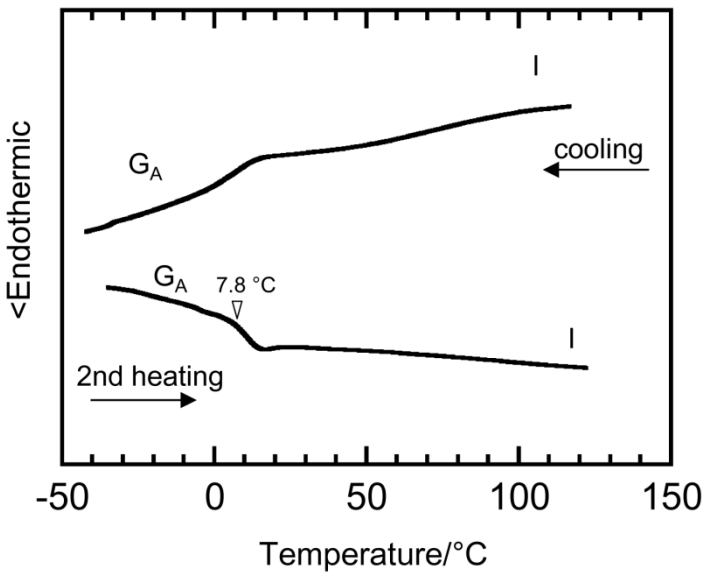

(b)

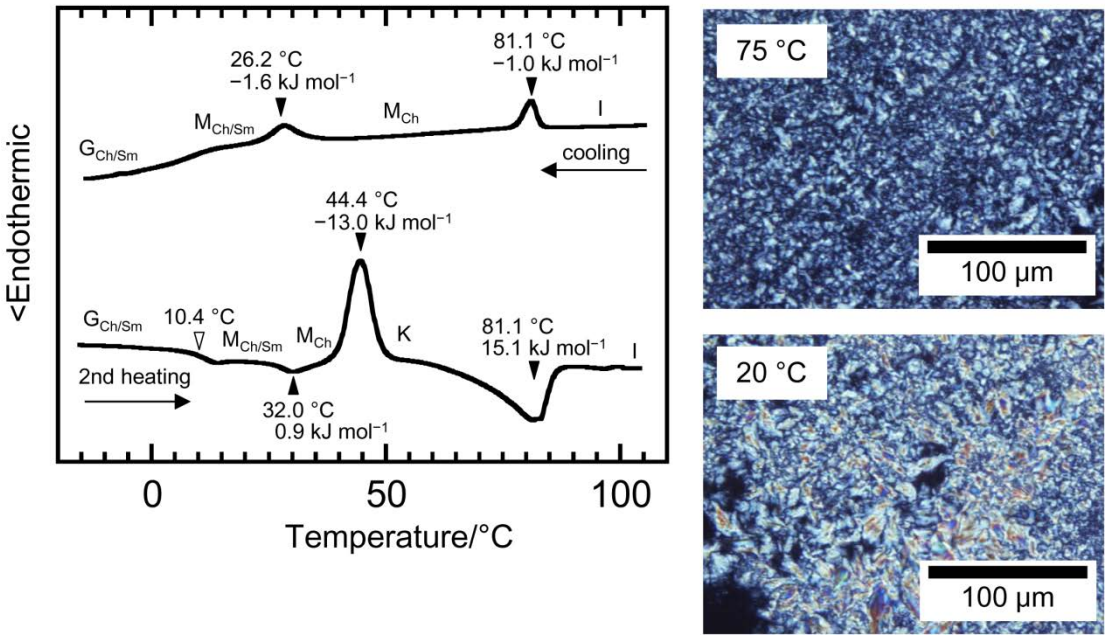

Figure 6

(c)

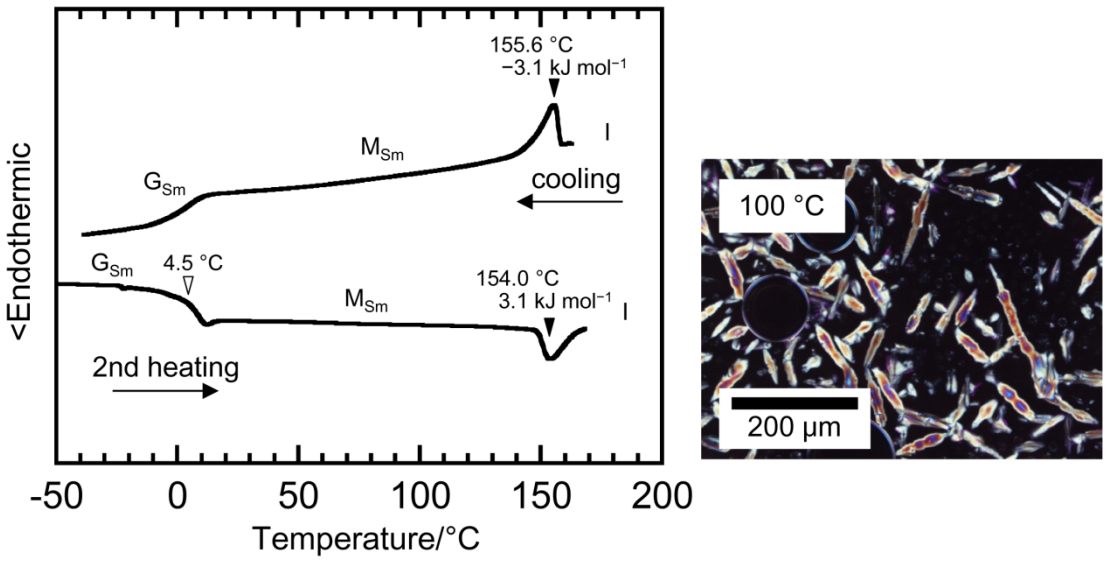

(d)

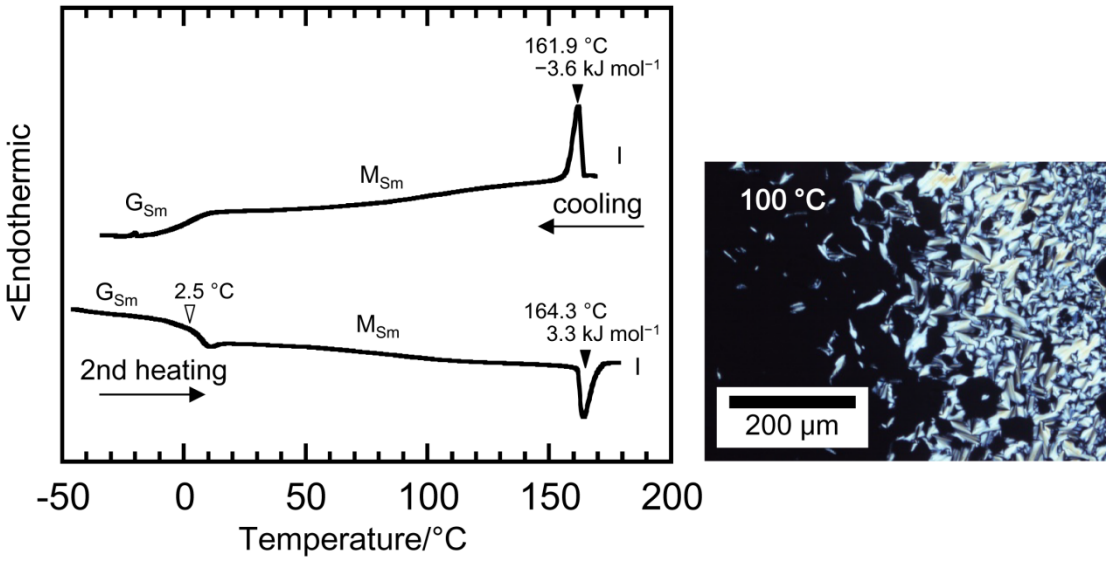

Figure 6 Continued.

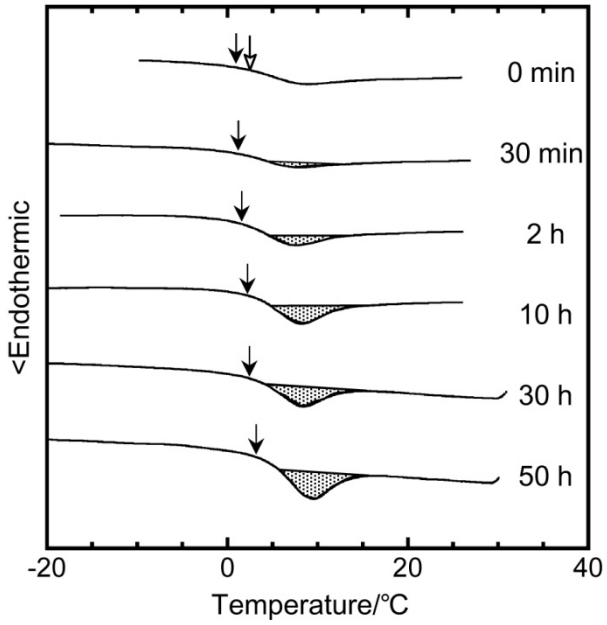

Figure 7

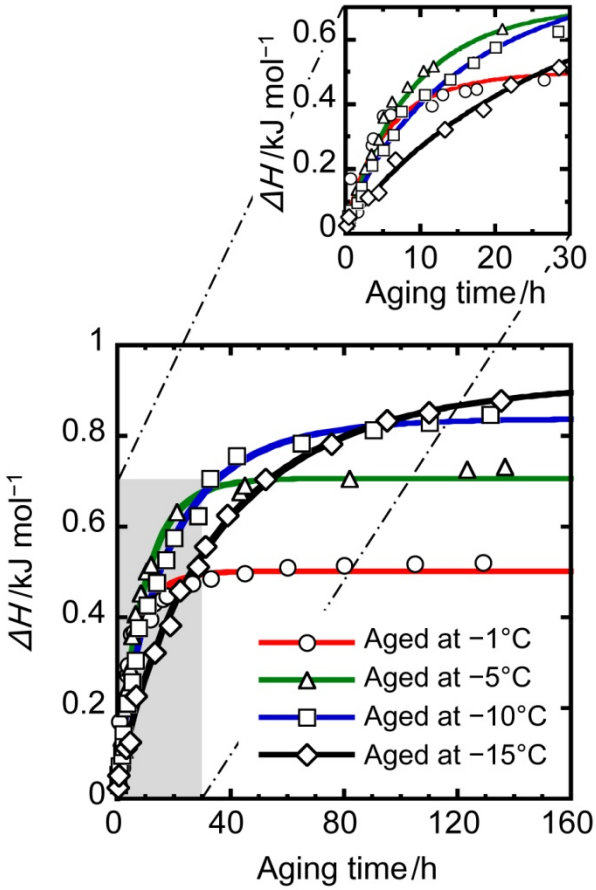

Figure 8

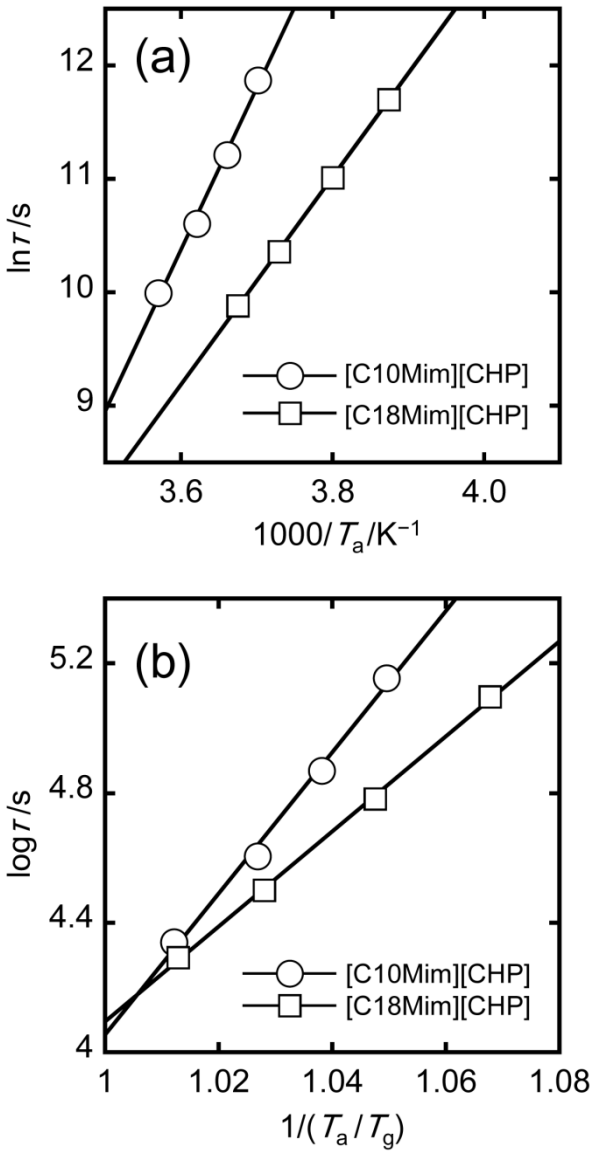

Figure 9

Table 1 Thermal transition property of CHP and [C*n*Mim][CHP] complexes

Sample	Phase transition pattern	Phase transition scheme	T_g[1)]/°C	T_{M-I}[1)]/°C	ΔH_{M-I}[1)] /kJ mol^{-1}
CHP *per se* [2)]	–	$G_{Ch} \leftrightarrow M_{Ch} \leftrightarrow I$	25.8	91.4	3.3
[C6Mim][CHP]	A	$G_A \leftrightarrow I$	13.9	–	–
[C8Mim][CHP]	A	$G_A \leftrightarrow I$	7.8	–	–
[C10Mim][CHP]	B	$G_{Ch/Sm} \leftrightarrow M_{Ch/Sm} \leftrightarrow M_{Ch} \leftarrow I$, $M_{Ch} \searrow \nearrow K$	10.4	81.1	– (1.0[3)])
[C12Mim][CHP]	B	$G_{Ch/Sm} \leftrightarrow M_{Ch/Sm} \leftarrow M_{Ch} \leftrightarrow I$, $M_{Ch/Sm} \searrow \nearrow K$	12.6	122.6	1.7 (1.8[3)])
[C14Mim][CHP]	C	$G_{Sm} \leftrightarrow M_{Sm} \leftrightarrow I$	4.5	154.0	3.1 (3.1[3)])
[C16Mim][CHP]	C	$G_{Sm} \leftrightarrow M_{Sm} \leftrightarrow I$	4.1	161.4	3.4 (3.4[3)])
[C18Mim][CHP]	C	$G_{Sm} \leftrightarrow M_{Sm} \leftrightarrow I$	2.5	164.3	3.3 (3.6[3)])

Abbreviations: K, crystal; M, mesophase; G, glassy state; A, amorphous; Ch, cholesteric; Sm, smectic. [1)] Estimated in the 2nd heating scan. [2)] Data were all quoted from ref. 8. [3)] Estimated in the cooling scan.

Table 2 Analytical results of enthalpy relaxation for LC glasses of CHP, [C*n*Mim][CHP], and comparable CHP/C*n*-amine complexes

Sample	T_g/°C	$T_g - T_a$ /°C	ΔH_∞ /kJ mol^{-1}	τ/s	lnτ/s	β	E_a /kJ mol^{-1}	m
CHP *per se*[1)]	25.8	18.8	1.83	2.51×10^{5}	12.40	0.69	154	27
		10.8	1.31	3.34×10^{4}	10.40	0.74		
		5.8	1.21	1.00×10^{4}	9.22	0.78		
		2.8	1.02	7.94×10^{3}	8.97	0.70		
[C10Mim][CHP]	10.4	13.4	1.59	1.43×10^{5}	11.87	0.96	118	22
		10.4	1.44	7.41×10^{4}	11.21	0.95		
		7.4	1.27	4.04×10^{4}	10.61	0.87		
		3.4	1.03	2.19×10^{4}	9.99	0.80		
[C18Mim][CHP]	2.5	17.5	0.919	1.25×10^{5}	11.70	0.85	76	15
		12.5	0.887	6.06×10^{4}	11.01	0.82		
		7.5	0.842	3.16×10^{4}	10.36	0.84		
		3.5	0.502	1.96×10^{4}	9.88	0.84		
CHP/C10-amine[2)]	18.7	16.7	1.69	9.17×10^{4}	11.4	0.87	94	17
		13.7	1.52	2.76×10^{4}	10.2	0.91		
		8.7	1.49	1.77×10^{4}	9.78	0.98		
		3.7	1.26	1.18×10^{4}	9.38	0.87		
CHP/C16-amine[1)]	19.0	19.0	0.849	1.51×10^{3}	7.32	0.98	52	9
		14.0	0.604	9.53×10^{2}	6.86	0.92		
		10.0	0.408	7.41×10^{2}	6.61	0.90		
		7.0	0.262	5.61×10^{2}	6.33	0.84		
CHP/C18-amine[1)]	20.0	25.5	0.990	2.37×10^{3}	7.77	1.00	47	8
		20.3	0.949	1.33×10^{3}	7.19	0.98		
		15.5	0.730	1.04×10^{3}	6.95	0.91		
		13.0	0.521	8.98×10^{2}	6.80	0.84		

[1)] Data are all quoted from ref. 9. [2)] Data are all quoted from ref. 10.